Phys. Med. Biol., 1990, Vol. 35, No 5, 679-685. Printed in the UK

Instrumental note

A technique for digital image registration used prior to subtraction of lung images in nuclear medicine

P A Kenny†, D J Dowsett†, D Vernon,‡ and J T Ennis†

† Institute of Radiological Sciences, Mater Misericordiae Hospital, 52 Eccles Street, Dublin 7, Ireland

‡ Department of Computer Science, Trinity College, Dublin 2, Ireland

Received 4 August 1989, in final form 11 January 1990

1. Introduction

In nuclear medicine, images of lung perfusion are routinely used to detect the presence of a pulmonary embolism. To confirm the diagnosis a ventilation scan is usually performed. Mismatches between the ventilation and perfusion images indicate a high probability of pulmonary embolism. Aerosols of ^{99m}Tc-labelled DTPA may be used to produce the ventilation image. One disadvantage of this technique is that ventilation imaging must either be performed before perfusion imaging or on the following day. A perfusion scan is best performed first since if this is normal no ventilation scan is required. A two day procedure delays diagnosis and may be logistically inconvenient when the patient has been referred from another hospital. If the perfusion images are abnormal, shown for a lung model in figure 1(a), then a ventilation scan may be requested. The image obtained after aerosol inhalation immediately after perfusion, figure 1(b), is a composite image of lung perfusion overlayed by ventilation. This occurs because both pharmaceuticals (MAA for perfusion and DTPA for ventilation) are labelled with ^{99m}Tc. In general the contribution from the ventilation to the total activity imaged is quite small (about 20–30%) and the composite image may appear very similar to the perfusion image. The ventilation image, figure 1(c), can be produced by a computer subtraction (Dowsett *et al* 1985) of the perfusion image from the composite image. A valid ventilation image will only be produced if the patient retains the same position in front of the γ camera during the perfusion imaging (1.5 min), aerosol inhalation (5 min) and imaging of the composite (1.5 min). Total counts acquired using this protocol are typically between 500–1000 k for the perfusion and 100–300 k for the subtracted ventilation image. Invariably artefacts are produced in the ventilation image obtained by subtraction, figure 1(d), due to patient movement.

The software solution involves digital image re-alignment of the two images prior to subtraction. Linear forms of digital image registration, orthogonal pixel shifting, (e.g. Dowsett and Perry 1970, Appledorn *et al* 1980), and image rotation, (e.g. Goris and Briandet 1983, Fleming 1984), are available on most modern nuclear medicine computers. Many of these implementations operate on a trial and error basis or with the use of marker sources. However, it cannot be assumed, when dealing with large organs such as the lungs, that the displacements between the images are purely linear.

Correspondence to: Mr P A Kenny

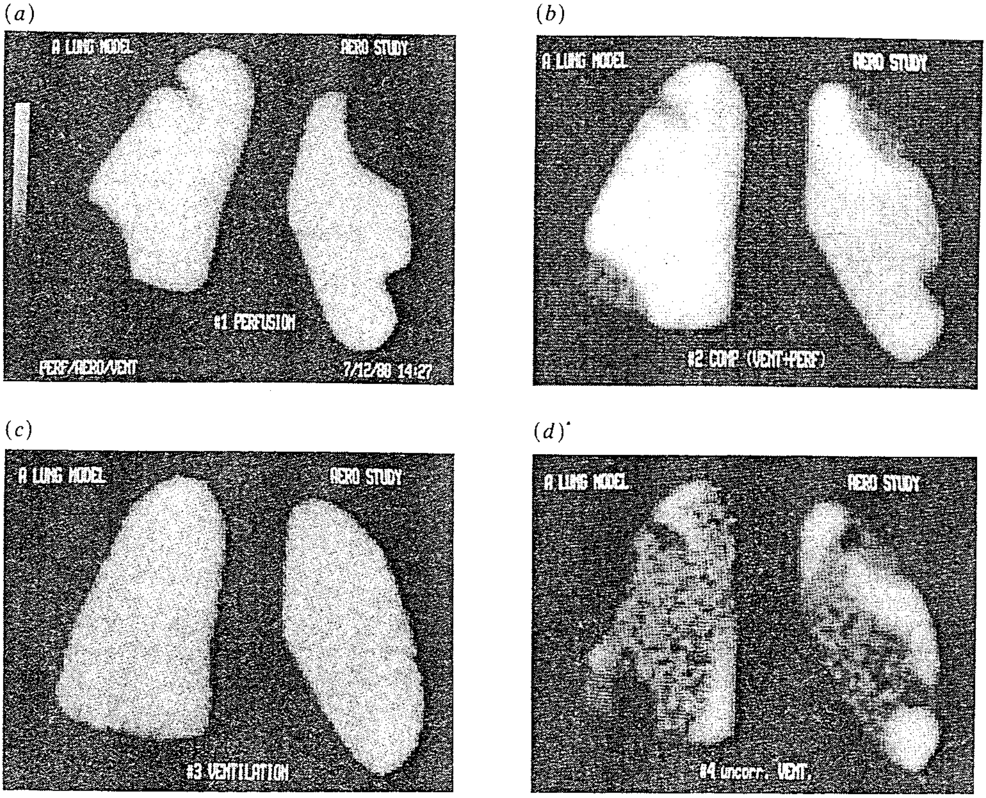

Figure 1. Principles of aerosol ventilation image formation immediately after perfusion for a lung model. (*a*) The perfusion image; (*b*) the composite image of perfusion overlayed by aerosol deposition; (*c*) the ventilation image obtained after computer subtraction of (*b*) from (*a*) with no patient movement introduced between image acquisition; and (*d*) artefacts introduced in the ventilation image due to patient movement.

The aim of the approach to image registration described here is to find a general relationship, described by polynomials, for the distribution of activity in the perfusion image compared to the distribution in the composite image of perfusion and ventilation. This technique was used because the actual spatial relationship between the lungs in both images will never be known prior to re-alignment. For each pair of images the spatial relationship is unique and is characterised by the coefficients of the polynomial expressions. The coefficients for each polynomial approximation are calculated using picture element locations (control points). These corresponding pairs are located manually at similar anatomical positions in both images with a user-guided screen cursor. The appropriate grey level for each pixel in the registered perfusion image is found in the original at coordinate locations which are returned by the polynomial expressions.

2. Description of the registration algorithm

Registration of two similar images, I and II, of some object (lungs), one of which may have received some unknown displacement of change in shape, requires that one of these images, say I, receives a non-linear spatial mapping so that every point in that image superimposes, i.e. maps, onto its corresponding point in II. Such a plane-to-plane non-linear mapping, $\boldsymbol{W}$, is normally referred to as a spatial warping function. For any given point in the registered image II, this function generates the coordinates of the corresponding point in the unregistered image I. This is shown in figure 2.

The relationship may be expressed by the equation

$$(Q_x, Q_y) = [\boldsymbol{W}_x(C_x, C_y), \boldsymbol{W}_y(C_x, C_y)] \tag{1}$$

where (C_x, C_y) is a registered pixel in the warped version of image I. This corresponds positionally to image II. The coordinate (Q_x, Q_y) is the corresponding unregistered pixel in image I. Thus, given any registered coordinates (C_x, C_y) in image II, the unregistered coordinates (Q_x, Q_y) in image I can be generated using the warping functions $\boldsymbol{W}_x$ and $\boldsymbol{W}_y$ respectively.

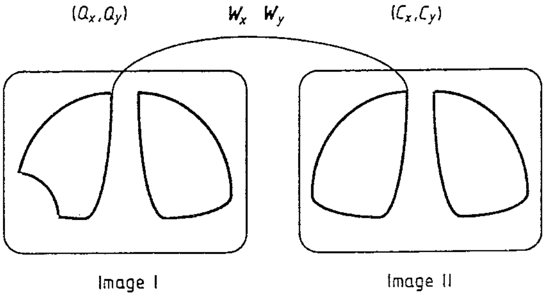

Figure 2. Mapping between image I, e.g. perfusion, and image II, e.g. composite aerosol image. The coordinates are related by the spatial warping functions $\boldsymbol{W}_x$ and $\boldsymbol{W}_y$.

Since analytical expressions for $\boldsymbol{W}_x$ and $\boldsymbol{W}_y$ cannot be known, a common approach is to model each spatial warping function by an nth-order polynomial in C_x and C_y (Pratt 1978) or by polynomials of the form (Hall 1979)

$$\sum_{ij}^{nn} \sum^{6} a_{ij} C_x^i C_y^j .$$

Now, $\boldsymbol{W}_x$ and $\boldsymbol{W}_y$ may be written

$$\boldsymbol{W}_x(C_x, C_y) = Q_x = \sum_{ij}^{nn} \sum a_{ij} C_x^i C_y^j \tag{2}$$

$$\boldsymbol{W}_y(C_x, C_y) = Q_y = \sum_{ij}^{nn} \sum b_{ij} C_x^i C_y^j \tag{3}$$

where a_{ij} and b_{ij} are the polynomial coefficients which characterise each mapping function between the images and n is the degree of the polynomial.

In order to model the (geometric) spatial warping, it is necessary merely to estimate the coefficients a_{ij} and b_{ij} of each polynomial. These can be determined by actually specifying the spatial warping for at least the same number of points in the images to be registered. This is accomplished by selecting pairs of corresponding 'control' points within each image.

A system of equations in a_{ij} and b_{ij} may be constructed. An exact system of equations occurs when the number of control point pairs equals the number of unknown polynomial coefficients. This can then be solved simultaneously to determine the coefficient vectors $\boldsymbol{A}$ and $\boldsymbol{B}$ of the spatial warping polynomial functions:

$$\boldsymbol{A} = \boldsymbol{U}^{-1} \cdot \boldsymbol{Q}_x \tag{4}$$

$$\boldsymbol{B} = \boldsymbol{U}^{-1} \cdot \boldsymbol{Q}_y. \tag{5}$$

$\boldsymbol{Q}_x$ and $\boldsymbol{Q}_y$ are the control point vectors in image I and $\boldsymbol{U}^{-1}$ is the inverse of the independent variable matrix derived from control points in image II.

The solution of an exact system of equations such as this is very sensitive to the choice of control point, however, and inappropriate choices can yield a poor model of the required spatial warping. This problem can be overcome by locating more control point pairs than there are polynomial coefficients. This produces an overdetermined system of equations (Pratt 1978, p 207). Unfortunately, in this case the independent variable matrix $\boldsymbol{U}$ (equations (4) and (5)) is no longer square and so its inverse $\boldsymbol{U}^{-1}$ cannot be computed. However it is possible to calculate a pseudo-inverse $\boldsymbol{U}^{+}$ (Ballard 1982), which minimises the mean square error between the control coordinates, $\boldsymbol{Q}_x$ and $\boldsymbol{Q}_y$, and their polynomial estimates given by $\boldsymbol{U} \cdot \boldsymbol{A}$ and $\boldsymbol{U} \cdot \boldsymbol{B}$ respectively. The system for the horizontal set of polynomial coefficients, for example, may now be written as

$$\boldsymbol{Q}_x = \boldsymbol{U} \cdot \boldsymbol{A} + \boldsymbol{E} \tag{6}$$

where the vector $\boldsymbol{E}$ represents the error between the observation coordinates and those obtained by polynomial estimation. This system is then solved for $\boldsymbol{A}$ subject to the condition that $\boldsymbol{E}^{\mathrm{t}}\boldsymbol{E}$ be a minimum, where $\boldsymbol{E}^{\mathrm{t}}$ is the matrix transpose $(E_{ij} \rightarrow E_{ij})$ of $\boldsymbol{E}$:

$$\boldsymbol{A} = (\boldsymbol{U}^{\mathrm{t}}\boldsymbol{U})^{-1}\boldsymbol{U}^{\mathrm{t}}\boldsymbol{Q}_x \tag{7}$$

$$\boldsymbol{A} = \boldsymbol{U}^{+} \cdot \boldsymbol{Q}_x. \tag{8}$$

This is repeated for the $\boldsymbol{B}$ (vertical) coefficient vector, where $\boldsymbol{U}^{+}$ is the pseudo-inverse of $\boldsymbol{U}$.

The elements of the coefficient vectors thus obtained characterise the particular mapping between the object in image I and image II. The final registered version of image I which should be spatially coincident with image II is generated by using 'pixel filling' (Castleman 1979 p 96). For each pixel location in the registered image, (C_x, C_y), the appropriate grey value for that pixel occurs at coordinates (Q_x, Q_y), obtained using equations (2) and (3) in the unregistered image I.

The values returned using the transformations represent grey-level coordinates in the unregistered image I and generally take non-integer values. Since grey values are only defined at integer locations some form of estimation of the grey levels in the registered version of I must be performed. First-order or bilinear interpolation (Castleman 1979 p 113) is used in this implementation. This calculates the grey level in the registered image as a weighted average of the grey levels at the four nearest coordinates in the original.

3. Results and discussion

The application of this warping technique to post-perfusion aerosol imaging of pulmonary ventilation has proved successful and the technique is in current clinical use.

The requirement that the patient remains still during inhalation of aerosol between image acquisition is no longer necessary. In fact, the patient may now be moved from the camera and the inhalation performed in an adjacent room; a composite perfusion/ventilation image is then acquired with small regard to accurate repositioning. Figure 3 demonstrates the improvement obtained on the lung model after spatially warping the perfusion image. Figure 4 shows the results obtained from a set of patient data imaged from the posterior.

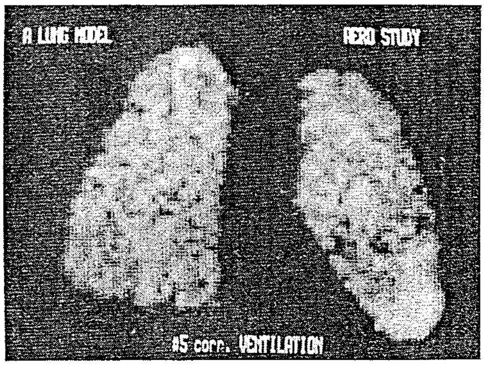

Figure 3. The ventilation image (obtained after spatially warping the perfusion image, shown in figure 1(a), prior to subtraction from figure 1(b)) shows a dramatic reduction in the amount of subtraction artefacts.

Ten and 14 pairs of control points have been used to calculate the coefficients for polynomials of four and six terms respectively. The accuracy of this technique rests, of course, on the selection of representative pairs of control points. This dependency is alleviated somewhat by over-determining the specification of the geometric transformation. This is particularly useful if gross differences exist between the images. In some situations these differences between the perfusion and aerosol composite images may of course be sufficient to confirm the diagnosis of pulmonary embolism and image subtraction may not be required.

It is highly desirable that the control point pairs are faithfully identified in both images. The precision of image registration is improved if images of the lung boundaries are used for the selection of control points. These points are typically situated at positions of high curvature on the boundary and must be present in both boundary images. Figure 5 shows the boundaries of the lung images shown in figure 4. They have been achieved using a method of edge detection based on image enhancement which does not require the specification of a threshold value (Marr and Hildreth 1980). The edges obtained using this technique are contours or boundaries which makes them amenable to further processing. The boundaries produced using Marr–Hildreth edge detection are reliable but the technique is computationally quite expensive.

Current research is directed towards automatic selection of the registration control points on the images of the lung boundaries. In the approach under investigation the boundaries are stored as chain codes (Freeman 1961). Coordinates corresponding to peaks in the curvature (derived from the chain codes) are isolated as control points.

It is invisaged that the use of spatial warping and its automation may have applications as a means of registering images from different diagnostic procedures prior to some comparative analysis, e.g. a nuclear medicine lung scan and a chest x-ray.

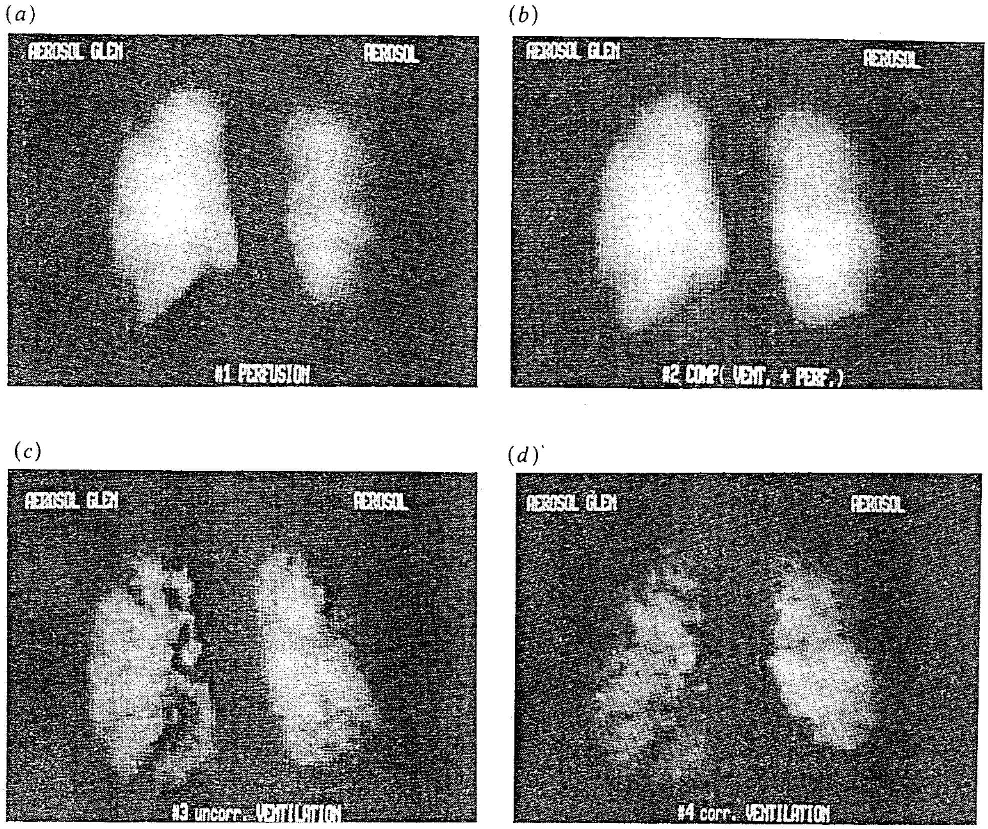

Figure 4. Patient data set, posterior view: (*a*) the perfusion image; (*b*) the composite image of perfusion overlayed by ventilation; (*c*) the ventilation image obtained by subtracting the unregistered perfusion image (*a*) from the composite image (*b*); and (*d*) the ventilation image obtained after image registration prior to subtraction. This patient was reported as having a high probability of pulmonary embolism.

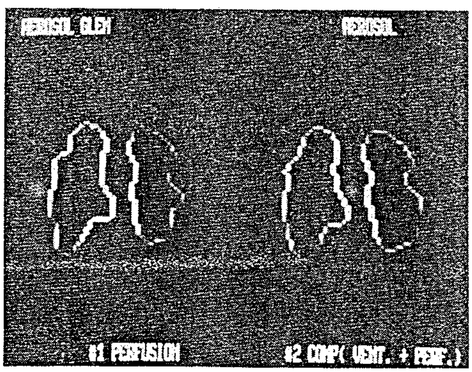

Figure 5. Lung boundaries of the patient data set obtained using Marr–Hildreth edge detection.

References

Appledorn C R, Oppenheim B E and Wellman H N 1980 An automated method for the alignment of image pairs *J. Nucl. Med.* **21** 165–7

Ballard D H and Brown C M 1982 *Computer Vision* (London: Prentice Hall) p 485

Castleman K R 1979 *Digital Image Processing* (New York: Wiley)

Dowsett D J, Kenny P A and Ennis J T 1985 Computer image subtraction gives separate lung perfusion and ventilation images using ^{99m}Tc-MAA and DTPA aerosols *Proc. European Nuclear Medicine Conf.*, London pp 225–30

Dowsett D J and Perry B J 1970 Automatic analysis of brain scan images *Br. J. Radiol.* **43** 617–20

Fleming J S 1984 A technique for motion correction in dynamic scintigraphy *Eur. J. Nucl. Med.* **9** 397

Freeman H 1961 On the encoding of arbitrary geometric configurations *IEEE Trans. Elec. Comput.* **EC-10** 260–4

Goris M L and Briandet P A 1983 *A Clinical and Mathematical Introduction to Computer Processing of Scintigraphic Images* (New York: Raven Press) pp 205–9

Hall E L 1979 *Computer Image Processing and Recognition* (New York: Academic Press) p 187–8

Marr D and Hildreth E C 1980 Theory of edge detection *Proc Royal Soc.* B **207** 187

Pratt W K 1978 *Digital Image Processing* (New York: Wiley) pp 429–31